Journal of Inorganic and General Chemistry
ZAAC
Zeitschrift für anorganische und allgemeine Chemie
DOI: 10.1002/zaac.202000275
ARTICLE

On the Reactivity of NHC^{tBu}AuCl towards $Rb_6Cs_6Si_{17}$: The First Gold-Silicon Cluster $[(NHC^{tBu}Au)_6(\eta^2\text{-}Si_4)]Cl_2{\cdot}7NH_3$ and an Imide Capped Gold Triangle $(NHC^{tBu}Au)_3NHCl$

Susanne M. Tiefenthaler,[a][‡] Verena Streitferdt,[b][‡] Josef Baumann,[a] Stefanie Gaertner,[a] Ruth M. Gschwind,[b] and Nikolaus Korber*[a]

Dedicated to Professor Bernd Harbrecht on the Occasion of his 70th Birthday

Abstract. Crystals of the two new compounds $(NHC^{tBu}Au)_3NHCl$ and $[(NHC^{tBu}Au)_6(\eta^2\text{-}Si_4)]Cl_2{\cdot}7NH_3$ could be isolated from the reaction of $Rb_6Cs_6Si_{17}$ with $NHC^{tBu}AuCl$ in the presence of [2.2.2]-cryptand in liquid ammonia. Both compounds were characterized by single-crystal X-ray diffraction and crystallize trigonally without any alkali metals or chelating ligands. Additionally, the crystal of $[(NHC^{tBu}Au)_6(\eta^2\text{-}Si_4)]Cl_2{\cdot}7NH_3$ was further interpreted by means of ELF and NBO calculations. In the case of $(NHC^{tBu}Au)_3NHCl$, NMR experiments provided an exceptional insight into the reaction processes in solution and allowed for the detection of sequential precursors. In the class of capped gold triangles $(NHC^{tBu}Au)_3NHCl$ impresses with its unique characteristics of being capped by an imide and bound to *N*-heterocyclic carbenes as ligands instead of the ubiquitously employed phosphines. The gold capped silicon tetrahedron $[(NHC^{tBu}Au)_6(\eta^2\text{-}Si_4)]Cl_2{\cdot}7NH_3$ represents the first known silicide-gold compound, as well as the first known functionalized Zintl anion, crystallized with a cationic central moiety.

Introduction

Gold is known to form intra-elemental bonds, especially in the oxidation state +1. This effect is commonly referred to as aurophilicity, since gold is the prime example of this interaction, even though it occurs in other late closed shell transition metals as well.[1] A well-known type of gold(I) phosphine complexes are gold triangles, often capped with a nitrogen atom, which is usually connected to an organic or metalorganic group.[2,3] Over the past few years, *N*-heterocyclic carbenes (NHC) gained interest as ligands in organometallic chemistry. Among NHC-transition metal complexes, those containing Au^I have proven great applicability in the fields of luminescence, medicinal chemistry and homogeneous catalysis.[4] NHC-Au^I complexes find also use in coordination to homoatomic polyanions of main group metals, also termed Zintl anions, which provide versatile reaction possibilities.[5] While homoatomic polyanions of germanium, tin and lead exhibit a rich coordination chemistry with transition metal complexes, only four examples of transition metal functionalized silicon clusters are known so far, starting with the publication of $[Si_9ZnPh]^{3-}$ by *Sevov* in 2006.[6] Since then, two additional compounds containing a functionalized $[Si_9]^{x-}$ moiety have been reported ($[\{Ni(CO)_2\}_2(\mu\text{-}Si_9)_2]^{8-}$ and $[NHC^{Dipp}Cu(\eta^4\text{-}Si_9)]^{3-}$),[7,8] as well as the mesitylcopper adduct $[(MesCu)_2Si_4]^{4-}$.[9] The latter represents the only known case of a tetrasilicide transition metal complex. Here, face capping of the tetrahedral anion by a 3d metal seems to be the most favorable coordination setting. Five compounds of functionalized Zintl ions containing gold – germanium bonds are known ($[Au_3Ge_{18}]^{5-}$, $[Au_3Ge_{45}]^{9-}$, $[(\eta^3\text{-}Ge\{Si(SiMe_3)_3\}_3)Au(NHC^{Dipp})]$, $[Au[Ge_9(Si(i\text{Bu})_3)_3]_2]^-$, and $[AuGe_{18}\{Si(SiMe_3)_3\}_6]^-$),[10] whereas literature only provides one example each for tin ($[NHC^{Dipp}Au(\eta^4\text{-}Sn_9)]^{3-}$) and lead ($[Au@Pb_{12}]^{3-}$).[11] Gold silicon compounds are promising materials, particularly on the nanoparticle scale.[12]

Despite the growing use of silicon Zintl ions, studies of Zintl ions in solution in general have only emerged in the last decade. NMR would be a suitable and non-destructive examination method, amongst others because of its applicability to a variety of different heteronuclei. However, NMR studies are particularly challenging due to the complex preparation of the samples as well as the low solubility of the initial (silicon) Zintl phases entailing resolution problems. Despite great efforts, many solvation and reaction processes remain still unknown. Nevertheless, in recent years we were able to detect novel silicides, naked,[13] as well as protonated,[14,15] in solutions of ammonia by means of multinuclear NMR spectroscopy and to show unexpected protonation and dynamic behavior. Reactions using complexes with a transition metal bound to aryl groups and, more recently, to NHCs have proven successful in the functionalization of silicide clusters, however,

[‡] These authors contributed equally to this work.
* Dr. N. Korber
E-Mail: Nikolaus.Korber@ur.de
[a] Institute of Inorganic Chemistry
University of Regensburg
93040 Regensburg, Germany
[b] Institute of Organic Chemistry
University of Regensburg
93040 Regensburg, Germany
Supporting information for this article is available on the WWW under **http://dx.doi.org/10.1002/zaac.202000275** or from the author.

Table 1. Crystallographic data and details of the structure determinations of $(NHC^{tBu}Au)_3NHCl$ (**1**) and $[(NHC^{tBu}Au)_6(\eta^2\text{-}Si_4)]Cl_2{\cdot}7NH_3$ (**2**).

	$(NHC^{tBu}Au)_3NHCl$ (**1**)	$[(NHC^{tBu}Au)_6(\eta^2\text{-}Si_4)]Cl_2{\cdot}7NH_3$ (**2**)
Composition	$C_{33}H_{61}Au_3ClN_7$	$C_{66}H_{120}Au_6Cl_{1.97}N_{19.02}Si_4$
M /g·mol^{-1}	1182.24	2544.27
Crystal system	trigonal	trigonal
Space group	*R*3	*P*$\bar{3}$1c
a /Å	16.2851(3)	14.1243(3)
b /Å	16.2851(3)	14.1243(3)
c /Å	12.9883(3)	26.6537(5)
α /°	90	90
β /°	90	90
γ /°	120	120
Volume /Å^3	2983.07(13)	4604.9(2)
Z	3	2
F(000) (e)	1686.0	2426.0
ρ_{calcd} /g·cm^{-3}	1.974	1.835
μ /mm^{-1}	11.136	9.676
2*Θ*-range for data collection /°	6.908 to 52.756	6.53 to 61.162
Reflections collected/independent	3753 / 2311	25958 / 4454
Data / restraints / parameters	2311 / 1 / 139	4454 / 0 / 161
Goodness-of-fit on F^2	1.035	1.050
Final *R* indices [$I > 2\sigma(I)$]	R_1 = 0.0148, wR_2 = 0.0353	R_1 = 0.0318, wR_2 = 0.0478
R indices (all data)	R_1 = 0.0148, wR_2 = 0.0353	R_1 = 0.0571, wR_2 = 0.0532
$R_{int.}$	0.014	0.0552
$\Delta\rho$ max, $\Delta\rho$ min /*e*·Å^{-3}	0.67 / –0.45	0.66 / –0.55
Flack parameter	–0.005(10)	

reactivity as well as structural studies in solution are still rare. In the case of gold functionalized silicides, no crystal structures are known, let alone studies in solution. By the herein investigated reactivity of silicide anions derived by dissolution of a phase with the nominal composition $Rb_6Cs_6Si_{17}$ towards the complex $NHC^{tBu}AuCl$, we were able to fill these gaps. Crystals of the compounds $(NHC^{tBu}Au)_3NHCl$, consisting of an imide capped NHC functionalized gold triangle, and $[(NHC^{tBu}Au)_6(\eta^2\text{-}Si_4)]Cl_2{\cdot}7NH_3$, the first gold functionalized silicide, were obtained. Thereby we could open up the field of NHC functionalized and imide capped gold triangles, as well as of gold functionalized silicides.

Results and Discussion

Crystallographic Investigations

Crystals with the compositions $(NHC^{tBu}Au)_3NHCl$ (**1**) and $[(NHC^{tBu}Au)_6(\eta^2\text{-}Si_4)]Cl_2{\cdot}7NH_3$ (**2**) were isolated from a liquid ammonia solution of $Rb_6Cs_6Si_{17}$, $NHC^{tBu}AuCl$ and [2.2.2]-cryptand, with **1** being the main product. The crystallographic data obtained by single-crystal X-ray diffractometry is listed in Table 1. The molecular unit of **1** consists of an imide capped triangle of gold atoms, each bound to an NHC^{tBu} fragment (Figure 1). Chloride and imide generate a charge of –3 which is compensated by a threefold positively charged $(NHC\text{-}Au)_3$ moiety. This corresponds well to the assumption of an oxidation number of +1 for each gold atom.[2,3]

While the gold atom and the NHC^{tBu} fragment are situated on a general position, the imide and chloride ion occupy the special position 3a of space group *R*3. The nitrogen atom is elevated above the plane of the gold triangle and the bond length between nitrogen and gold (2.026(3) Å) is slightly

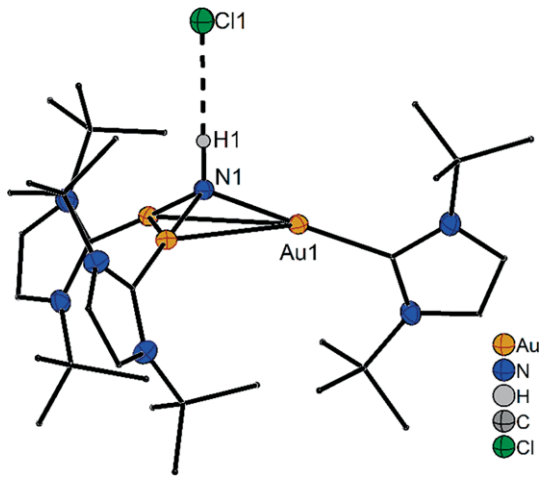

Figure 1. Formular unit of **1**. Hydrogen atoms are omitted and carbon atoms displayed as wires/sticks for added visibility; thermal displacement ellipsoids are drawn with 50 % probability.

shorter than in known structures.[2] The gold-gold distance is in the range of aurophilic bonds with a length of 3.2598(3) Å.[1] The chloride is surrounded by 13 hydrogen bonds in total, with bond lengths ranging from 2.424 to 3.858 Å. To summarize, we were able to isolate crystals of the first example of an NHC functionalized gold(I) triangle capped by an imide. $[NHC^{tBu}Au]^+$ can be looked upon as being isolobal to H^+, consequently compound **1** can be considered a heavy derivative of ammonium chloride.

The central moiety in the compound $[(NHC^{tBu}Au)_6(\eta^2\text{-}Si_4)]Cl_2{\cdot}7NH_3$ (**2**) is a silicon tetrahedron with a $NHC^{tBu}Au$ fragment capping each edge (Figure 2). A 50:50 disorder is present in the structure, giving the silicon center the appear-

ance of a cube. This cube is comprised of two interlocked tetrahedra, each present in the structure with 50 % occupation. This 50 % disorder is even present in *P*1, therefore the description in $P\bar{3}1c$ is correct. The two symmetrically independent Si–Si bond lengths are slightly elongated with 2.530(3) Å and 2.537(4) Å, in comparison to the bonds in the naked $[Si_4]^{4-}$ with lengths between 2.4032 Å and 2.4329 Å.[16] The phenomenon of the elongation of a capped edge is also known from the cluster $[HSi_4]^{3-}$, recently reported by us,[14] from $[(\mu_2\text{-H})(\eta^2\text{-Ge}_4)ZnPh_2]^{3-}$ reported by *Fässler* et al.,[17] as well as from $(t\text{Bu}_3\text{Si})_4\text{Si}_4$.[18] The Si–Au bond lengths range from 2.4020(3) Å to 2.412(2) Å and are therefore in between the length of a silicon-nickel (2.3 Å)[7] and a silicon-copper bond (2.43 Å).[8,9] Incidentally, this distance is the exact sum of the single bond radii calculated by *Pyykkö*.[19]

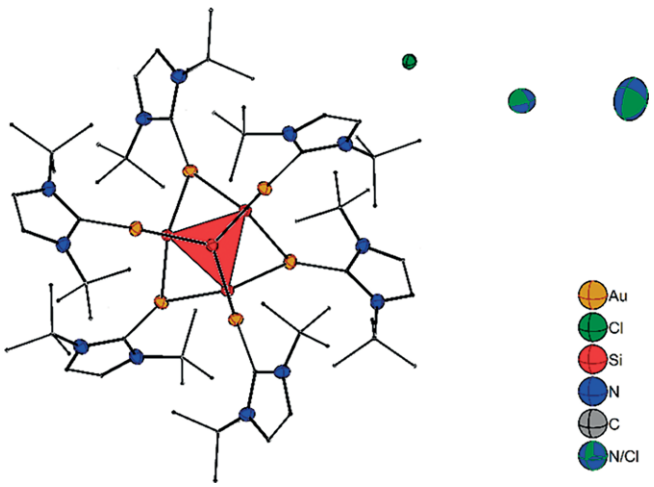

Figure 2. Formular unit of **2**. Hydrogen atoms are omitted and carbon atoms are displayed as wires/sticks for added visibility; thermal displacement ellipsoids are drawn with 50 % probability.

Since the oxidation state of gold in $NHC^{t\text{Bu}}AuCl$ is +1, as well as in the fragments in compound **1**, we assume a charge of +1 for each $NHC^{t\text{Bu}}Au$ fragment in compound **2**. This assumption leads us to assign a total charge of +2 to the central moiety $[(NHC^{t\text{Bu}}Au)_6(\eta^2\text{-Si}_4)]$ (**2A**), as the involved $[Si]_4$ cluster retains its fourfold negative charge.

In addition to the gold-silicon moiety, only three other crystallographically independent positions are present. Of these positions, only one can unequivocally be determined to be a chlorine atom (Cl1). We presume a charge of –1 for this atom, assigning it to be a chloride ion which results in a charge balance of +1. The remaining two atoms are on the special positions 12*i* and 4*f* respectively, leading to eight symmetry-generated positions. For these remaining eight positions, mixed occupied sites involving ammonia and chloride were realized resulting in an overall single negative charge (see Supporting Information). Together with Cl1 the twofold positive charge is balanced. This model is also strongly supported by the observed thermal stability of the crystal, as the cell could still be determined after several minutes at room temperature, despite the known extreme thermal instability of ammoniates due to the evaporation of ammonia. This might be an indication for additional strong interactions between Cl^- and NH_3, keeping the ammonia in the crystal, due to strong ion dipole interactions.

Similar to compound **1**, the central moiety can be seen as a heavier derivative of an unknown $[Si_4H_6]^{2+}$, considering the isolobal analogy between $[NHC^{t\text{Bu}}Au]^+$ and a proton. Interestingly though, calculations predicted an open structure for $[Si_4H_6]^{2+}$, and not, as it is the case in **2a**, a tetrahedron.[20]

Theoretical Calculations

Since the charge of the gold-silicon moiety could not be determined unequivocally based on the crystallographic data, calculations were performed to clarify the charge situation. Due to the high number of atoms and the amount of electrons from the gold atoms, the *tert*-butyl groups were replaced by methyl groups. In order to confirm the charge of +2, geometry optimizations (BP86/def2-TZVPP, CPCM = ammonia) were carried out assigning different charges +2, 0 and –4 to the cluster (see SI). The optimized geometries show a tetrahedral Si_4 moiety only in the case of the twofold positively charged compound. The exact calculated values for bond lengths and angles are listed in Table SI1 (Supporting Information).

A study of the isosurface from ELF (Electron Localization Function) calculation on $[Si_4(Au^{Me}NHC)_6]^{2+}$ shows a tetrasynaptic basin in the center of the Si tetrahedron (Figure 3). With a population of 1.57 electrons, it can be interpreted as a four-center bond. Furthermore, there are no attractors between two silicon atoms but between each silicon atom and its three neighboring gold atoms. These basins are populated with 0.8 electrons each.

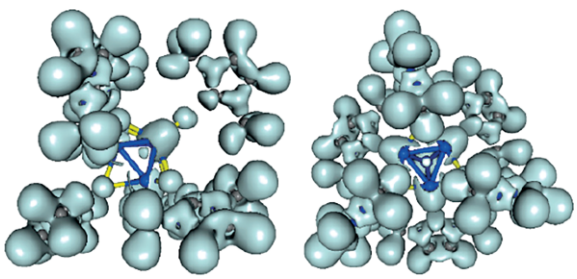

Figure 3. ELF isosurface of $[(NHC^{t\text{Bu}}Au)_6(\eta^2\text{-Si}_4)]^{2+}$ with η = 0.67; blue atoms represent silicon, yellow bonds lead to gold atoms.

Calculating the NPA of the cluster atoms with BP86/def2-TZVPP level of theory results in a negative charge of –0.53 at the Si atoms and a positive charge of +0.39 at every Au atom. The Au–C bonds are nearly fully occupied with 1.94062 electrons. Looking at the hybridization, one can notice the quite low contribution of d-orbitals in the Si lone pairs ($sp^{0.27}d^{0.01}$), Si-Si- bonds ($sp^{12.8}d^{0.27}$) and Au–C bonds (Au: $sd^{0.08}$, C: $sp^{1.6}d^{0.01}$). The Au-*NHC* fragments and the Si_4 tetrahedron are treated separately by NBO. Studying the second order perturbation, however, shows substantial stabilization energy due to electron delocalization from the Si–Si bond to the antibonding Au–C bond. This corresponds to the side-on coordination of the tetrahedron to the adjacent Au-*NHC* fragments (see Supporting Information).

In the case of germanium, recently the compound $[(\mu_2\text{-H})(\eta^2\text{-Ge}_4)\text{ZnPh}_2]^{3-}$ has been reported by *Fässler* et al., in which functionalization, as well as protonation occurs edge-on.[17] For silicon, so far no compound with a transition metal ligand capping the edge of a tetrahedron has been published. However, in 2018 a structure for protonated P_4 was published, showing the edge-on protonation of the compound, which is electronically comparable to $[Si_4]^{4-}$, according to the pseudo-electron concept.[21]

In conclusion, the crystallographic studies, as well as the calculations suggest the charge of **2A** as twofold positive. Compound **2** is unique in three ways, as it not only represents the first gold-functionalized silicide but also the first silicon Zintl cluster the edges of which are capped by transition metal ligands. Moreover, it represents the first known example of a cationic moiety crystallized from ammonia which contains a functionalized Zintl ion.

NMR Studies

In recent years, we were able to discover fascinating new silicides (Si_4^{4-}, HSi_9^{3-}, HSi_4^{3-}, and Si_5^{2-}) in solutions of $K_6Rb_6Si_{17}$ in liquid ammonia by means of NMR spectroscopy. Hence, we were curious which species would arise in a solution of $K_6Rb_6Si_{17}$ in presence of the gold complex NHC$^{t\text{Bu}}$AuCl. To increase solubility for NMR spectroscopic investigation in liquid ammonia, $K_6Rb_6Si_{17}$ instead of $Cs_6Rb_6Si_{17}$ was applied and [2.2.2]-cryptand was added.[22] In the following, based on the NMR spectroscopic examination of three samples (**i–iii**), first possible structures of the species detected in solution are discussed and a potential reaction mechanism to **1** is presented. Thereupon follows the analysis of a ^{1}H-NMR reaction monitoring and finally the presence of silicides in solution is examined. We started our investigations with a sample of silicide, gold complex and cryptand in a 1:1:1.5 ratio (sample **i**). One hour after preparation of the colorless mixture, the reaction was followed by ^{1}H-NMR at 233 K (see Figure 4).

The ^{1}H-NMR monitoring revealed the formation of various species containing the ligand NHC$^{t\text{Bu}}$. Due to the structure of the ligand and the resulting complexes, exclusively chemical shifts can be used for the assignment of the species. Yet, 2D ^{1}H-^{13}C-HSQC, -HMQC and -HMBC, ^{1}H-^{15}N-HSQC, ^{1}H-^{1}H-NOESY, ^{1}H-DOSY together with 1D ^{1}H signal monitoring and integration enabled the assignment of the majority of the signals, even though being almost exclusively singlets (see Figure 4 left). Carbenic carbons, denoted as C^2, exhibit distinctly different ^{13}C-NMR shifts depending especially on the type of their substituent. For C^2 connected to Au^I chemical shifts between 156 ppm and 200 ppm are reported,[23–26] while C^2 of the free NHC$^{t\text{Bu}}$ carbene appears at a higher ^{13}C-NMR shift of around 213 ppm.[26,27] The C^2 shift of the corresponding

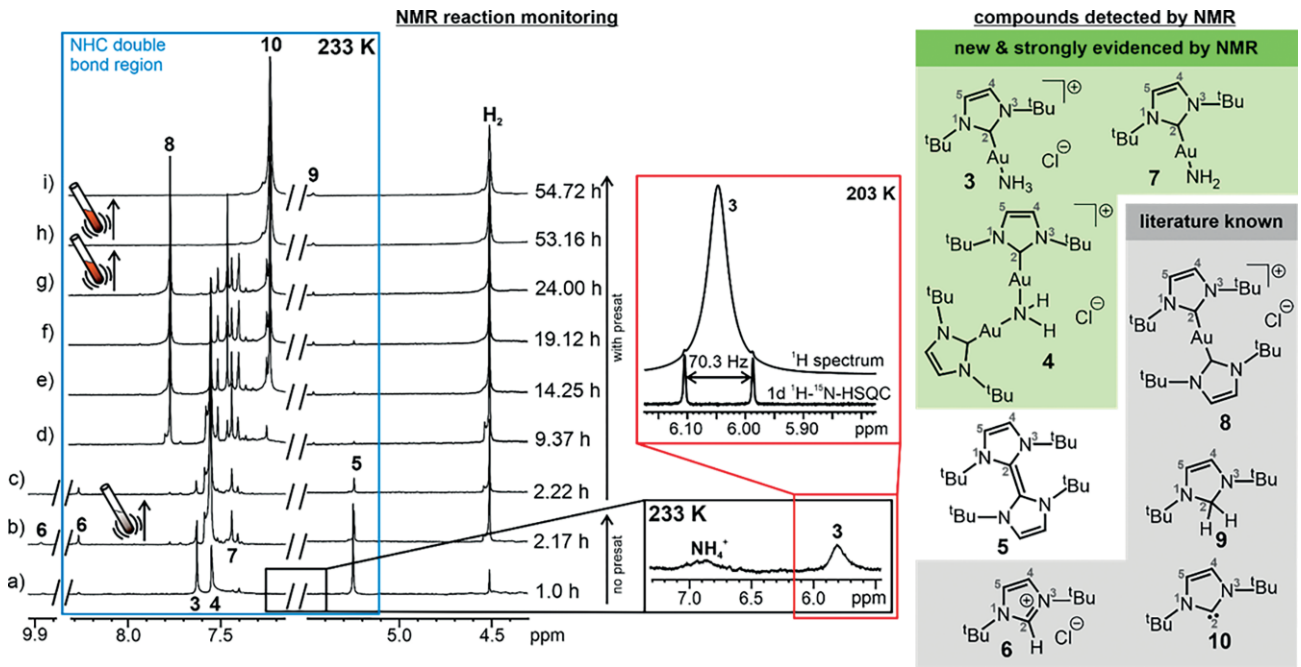

Figure 4. Left: ^{1}H-NMR reaction monitoring of a mixture of $K_6Rb_6Si_{17}$ (1 equiv.), NHC$^{t\text{Bu}}$AuCl (1 equiv.) and [2.2.2]-cryptand (1.5 equiv.) in liquid ammonia at 233 K reveals several reaction intermediates and their sequence. For spectra (a) and (b) solvent saturation was switched off to enable the detection of intermediates which exchange with NH_3 such as **3** and NH_4^+; for spectra (c) – (i) solvent saturation was switched on to increase sensitivity for the detection of small intermediates such as **9**. NMR tubes with lines of motion indicate shaking of the NMR tube. (In the light of past experience, the presence of Zintl ions in solution was usually associated with a coloration of the solution. Hence, by shaking the colorless sample from time to time, we hoped for dissolution of Zintl ions.) Middle bottom: spectral zoom of (a) of the not displayed region. Middle top: stacked spectra (standard ^{1}H-NMR spectrum and 1D ^{1}H-^{15}N-HSQC) of the ^{1}H-NMR region of N*H*$_3$ of **3** in sample **iii** at 203 K. Right: Compounds detected throughout the NMR spectroscopic investigation of samples **i–iii**. Structures, strongly evidenced by NMR, are highlighted by boxes. The structure of signal **5** can only be tentatively assigned since spectroscopical evidence was limited.

$NHC^{tBu}H^+Cl^-$ salt is reported at δ = 135.5 ppm,[27] whereas shifts of dihydro NHC species such as $NHC^{tBu}H_2$ and $(NHC^{tBu})_2H_2$ are reported at much lower values, i.e. between 63 and 91 ppm.[28,29] Consequently, the chemical shift of the carbenic carbon C^2 was a key factor for the following assignments. In case of L^1-Au^I-L^2 complexes, the connectivity between those ligands was indicated either via signal monitoring and integration or via ^{1}H-^{1}H-NOESY. A sample with a slightly different ratio of $K_6Rb_6Si_{17}$ to NHC^{tBu}AuCl and [2.2.2]-cryptand (1:2:2; sample **ii**) was found to react considerably slower than sample **i** (1:1:1.5 ratio) while generating mainly the same NHC species (see Supporting Information for exemplary spectrum) allowing for in-depth NMR investigations at 233 K and lower temperatures down to 203 K.

Structural Assignments

The majority of the signals emerging during the ^{1}H-NMR reaction monitoring displayed in Figure 4 were assigned by a combined investigation of the samples **i** and **ii** as well as a sample consisting solely of NHC^{tBu}AuCl in liquid ammonia (sample **iii**).

Of particular note is the detection and assignment of the complexes NHC^{tBu}-Au^I-$NH_3^+Cl^-$ (**3**) and $[(NHC\text{-}Au^I)_2\text{-}NH_2]^+Cl^-$ (**4**) (see Figure 4), both of which were yet unknown to literature. Only for **3** a similar copper complex $NHC^{Dipp}Cu\text{-}NH_3^+BF_4^-$ has been reported,[30] which may support the structural assignment of **3**. For **4**, there exists a hydroxyl analogue [NHCAu-OH-AuNHC][BF_4] which is used as catalyst in organic chemistry.[31] Key chemical shifts such as the ^{13}C-NMR shifts of C^2 (δ =166 ppm for **3** and 168 ppm for **4**) were used to identify the coordination of NHC to Au^I. The existence of NH_3 and NH_2 moieties in **3** and **4** were elucidated by ^{1}H-^{15}N-HSQC experiments and integration (see Figure 4 bottom right and Supporting Information). The associated ^{1}H-NMR signals of H^4 and H^5 at double bond (see Figure 4) followed the intensity pattern of NH_3 in **3** and NH_2 in **4**. In the case of complex **4**, this relation was confirmed by an NOE crosspeak. Furthermore, ^{1}H-DOSY (diffusion ordered spectroscopy) experiments revealed a larger hydrodynamic radius of **4** compared to **3** supporting their structures (see Supporting Information for more information on DOSY).

Considering the structures of **3**, **4** and **1** (see Figure 1 and Figure 4), **3** might be the structural precursor of **4** and **4** might be the precursor of **1**. The other signals could be assigned to structures **6**, **8**, **9** and **10** (see Figure 4) with the help of the existing literature.[23,27,28,32] A crystal structure for compound **8** could be determined from a separate reaction containing tin (for details, see Supporting Information). The structure belonging to the signal at δ = 5.25 ppm could only be guessed as NHC^{tBu} dimer (**5**) based on the assumption of an existing Wanzlick equilibrium between the NHC and its dimer[33] and upon comparison of its ^{1}H-NMR shift with literature values (see Supporting Information).[34] For **7** (see Figure 4) ^{1}H-^{1}H-EXSY and ^{1}H-DOSY experiments evinced that this compound is in chemical exchange with **3** and of similar size. From a chemical point of view and with regard to an assumed exchange via protonation/deprotonation, we considered NHC^{tBu}-Au-NH_2 (**7**) as an appropriate exchange partner (for EXSY studies see Discussion below and Scheme 2; for further data see Supporting Information).

Proposed Mechanism towards the Formation of 1

The ^{1}H-NMR signals of the starting material NHC^{tBu}-AuCl (H^4, H^5 at δ = 7.12 ppm [24]) have never been observed even in freshly prepared samples. Instead of NHC^{tBu}-AuCl, **3** and **4** were detected in all samples. This indicates a fast ligand exchange from Cl^- to NH_3 on gold due to the enormous excess of NH_3 (see Scheme 1a), which provides the first precursor **3** in the formation of crystal **1**. As the next step, we propose a chemical equilibrium between **3** and **7** as indicated by proton exchange in EXSY experiments (Scheme 1b). The detected intermediates provide several pathways for the abstracted protons. NH_4^+ (see Figure 4 middle and discussion below) and the generation of **6** hint at trapping by the solvent NH_3 or by the NHC^{tBu} carbene **10**. H_2 and **9** indicate the transformation of protons into hydrides (H^-) via oxidation of silicides (for the presence of silicides see discussion below; for the discussion of a trapping by Au species see Supporting Information). Next, complex **4** can be formed from **3** via a ligand exchange of NH_3 by **7** (c). For the further reaction pathway towards **1**, no additional intermediates could be detected. However, a repetition of the discussed reaction Scheme directly leads to the formation of **1**. Formal abstraction of HCl from **4** leads to **11**. Next again complex **1** can be formed from **3** via a ligand exchange of NH_3 by **11**(e).[35] Therefore, we assume the proposed reaction mechanism in Scheme 1 to be highly probable.

Next, the reaction monitoring was analyzed in light of the proposed mechanism. Due to the limited solubility of most of the intermediates (see Figure SI28 for evidence, Supporting Information), only the sequence of the intermediates can be interpreted. Indeed, in accordance with our mechanism, after one hour, a remarkable decrease of complex **3** was observed while the signals of **4** and **7** increased (see Figure 4b). Furthermore, after about 9 hours, the precursor **3** and the $NHC^{tBu}H^+Cl^-$ salt **6** disappeared and a significant signal of NHC^{tBu}-Au-$NHC^{tBu+}Cl^-$ **8** emerged confirming the principle possibility of ligand exchange NH_3 vs. NHC^{tBu}.

Without silicides the reaction stops at **3** as main species accompanied by small amounts of **4**, **6** and **8** (even up to one year at 193 K). This shows that the presence of silicides seems to be important for the reaction progress, most probably due to their potential to transform protons for further interactions. This deviates from other previous reports, in which ammonia can easily be fully aurated.[36] E.g. for R_3P ligands instead of NHCs on gold (I) the full auration can be obtained under suitable reaction conditions.[37]

Beyond the proposed mechanism, some additional observations are interesting. About 14 hours after sample preparation, the signal of free carbene **10** appeared (see Figure 4e). One day after preparation (Figure 4g), the NMR tube was shaken causing the supernatant to turn orange typical for dissolved silicides. In addition, the signals of the NHC^{tBu}-Au-species

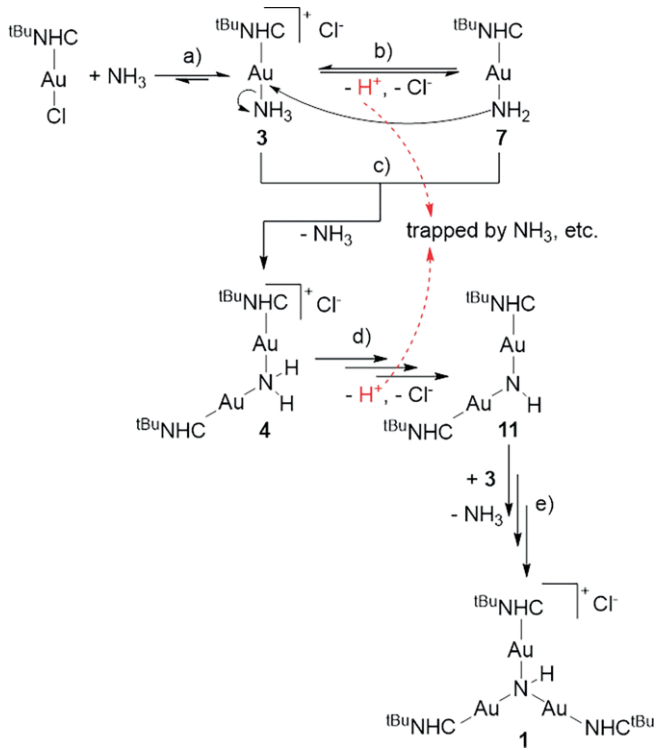

Scheme 1. Proposed mechanism for the formation of crystal **1** in solution.

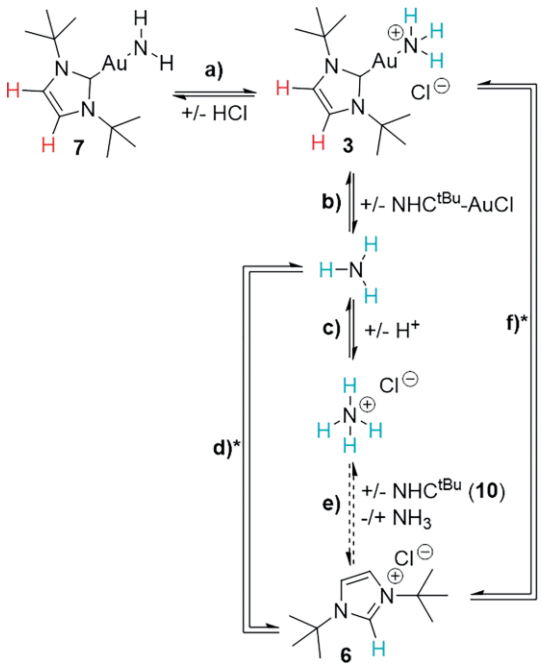

Scheme 2. Observed chemical exchange matrix from EXSY cross peaks. The exchange between ammonia and **3**, as well as between **3** and **7** corroborate parts of the proposed reaction mechanism. Asterisks indicate EXSY crosspeaks, which are assumed to be multistep exchange peaks. The exchange e) is below the detection limit most due to the low signal intensities of **6** and ammonium.

vanished and only the free carbene remained (see Figure 4i). Via ^{29}Si-NMR we could observe that the shaking really dissolved significant amounts of silicides (see below and Figure SI32, Supporting Information) which seem to change drastically the solubility of the gold complexes.

Chemical Exchange and ^{29}Si Studies

Next saturation transfer and EXSY experiments were used to gain insight into the chemical equilibria in solution. **3** exchanges with **7**, NH_3, and **6**. Furthermore, NH_3 exchanges with NH_4^+ and **6**.[40] The exchange between **3** and **7** (Scheme 2a) corroborates the second step in the proposed mechanism (see Scheme 1b). The exchange of **3** with NH_3 (see Scheme 2b) supports both the feasibility of ligand exchange on Au and the structure of **3**. At first glance the detected chemical exchange between NH_3 and **6** (Scheme 2d) seems to be unlikely, however we assume a multistep exchange over NH_4^+ (Scheme 2c, e; the direct exchange between ammonium and **6** is below the detection limit). This is in line with the detected exchange between **6** and **3** (see Scheme 2f), which is one step further in the multistep exchange between **6** and NH_3 (see Supporting Information for an in-depth investigation).

Finally, ^{29}Si-NMR experiments were used to gain insight into the silicide species present during this reaction. For the sample shown in Figure 4, only after 24 h and shaking of the sample silicides could be detected (without shaking also after 24 h no silicides can be observed). Then, the well-known degradation product H_3Si^-,[13,41] as well as the literature known protonated silicide $[HSi_9]^{3-}$ were detected (see Figures SI30–SI32 for spectra, Supporting Information).[15] Besides, 1D ^{29}Si spectra showed a couple of broad signals in the range between –300 and –360 ppm without coupling pattern, which could not be assigned (see Figure SI32a, Supporting Information). Nonetheless also below NMR detectability the silicides seem to play a key role since the reaction progress stops mainly at **3** without silicides present.

Overall, our combined NMR investigations of three samples (**i–iii**) allowed for the detection of the sequential structural precursors **3** and **4** of crystal **1** in solution. Furthermore, an exchange matrix and a plausible mechanism for the formation of crystal **1** could be postulated upon experimental evidence obtained by NMR spectroscopy.

Conclusions

Single crystal X-ray diffractometry of two different crystals obtained from a reaction of $Rb_6Cs_6Si_{17}$ with NHC^{tBu}AuCl in presence of [2.2.2]-cryptand in liquid ammonia revealed two new structures: $(NHC^{tBu}Au)_3NHCl$ (**1**) and $[(NHC^{tBu}Au)_6(\eta^2\text{-}Si_4)]Cl_2{\cdot}7NH_3$ (**2**). The compound $(NHC^{tBu}Au)_3NHCl$ (**1**) represents a first in its class of complex, as, while the motif of a nitrogen capped gold triangle is quite well known, no species with an imide has ever been reported. Furthermore, instead of NHC fragments being bound to the gold atoms, generally a phosphine ligand is in place. In case of **2**, crystal structure determination and calculations suggested a silicon tetrahedron capped with six NHC^{tBu}Au fragments on the edges with a total charge of +2. In addition to being only the fifth reported metal

functionalized silicide, **2** represents the first gold-functionalized silicide and also the first silicon cluster with edge-capping by transition metal ligands. Furthermore, it is the first reported crystal structure with a cationic central moiety, comprised of a functionalized silicon cluster.

^{1}H-NMR reaction monitoring of samples containing $K_6Rb_6Si_{17}$, NHC^{tBu}-Au-Cl and [2.2.2]-cryptand in liquid ammonia together with various 2D NMR experiments allowed for the detection and characterization inter alia of NHC^{tBu}Au-NH_3^+ (**3**) and (NHC^{tBu}Au)$_2$-NH_2^+ (**4**), two potential precursors in the formation of crystal **1**. Moreover, we could demonstrate that ammonia is not an innocent solvent, since it is involved in Brønsted acid-base equilibria with NHC-carbenes and in association-dissociation equilibria with NHC-Au complexes considerably influencing the product outcome. Furthermore, based on our NMR studies, we could postulate a mechanism towards the formation of crystal **1** and understand the quantity distribution of crystals **1** and **2**.

Experimental Section

All operations were carried out under argon atmosphere, either in a glovebox or with the help of Schlenk techniques. Liquid ammonia was dried and stored over sodium and cooled with a dry ice/ethanol mixture. The alkali metals were synthesized by reaction of the respective chloride with calcium and subsequently purified by distillation.

Synthesis of $Rb_6Cs_6Si_{17}$: The phase was synthesized by solid-state reaction techniques. Elemental rubidium (717.1 mg, 8.39 mmol), caesium (1115.2 mg, 8.39 mmol) and silicon (667.7 mg, 23.77 mmol) were put into a tantalum ampoule that was subsequently welded shut and jacketed in a fused silica ampoule. The ampoule was heated to 1223 K at a rate of 25 K/h, held at that temperature for two hours and consequently cooled to room temperature at 20 K·h^{-1}. The brittle, black reaction product was isolated and stored in an argon filled glovebox and characterized by powder X-ray diffraction and Raman spectroscopy.

Synthesis of $K_6Rb_6{}^{29}Si_{17}$ (100 % enriched): The phase was synthesized by solid-state reaction techniques. Elemental potassium (119.1 mg, 3.05 mmol), rubidium (260.3 mg, 3.05 mmol) and enriched silicon (250.0 mg, 8.63 mmol) were put into a tantalum ampoule that was subsequently welded shut and jacketed in a fused silica ampoule. The ampoule was heated to 973 K at a rate of 25 K/h, held at that temperature for 24 hours and consequently cooled to room temperature at 20 K·h^{-1}. The brittle, black reaction product was isolated and stored in an argon filled glovebox and characterized by powder X-ray diffraction and Raman spectroscopy. $K_6Rb_6{}^{29}Si_{17}$ (10 mg, 0.01 mmol), NHC^{tBu}AuCl (4.6 mg, 0.01 mmol or 9.2 mg, 0.02 mmol) and [2.2.2]-cryptand (4.6 mg, 0.015 mmol or 6.1 mg, 0.02 mmol) were weighed into heated heavy wall precision NMR sample tubes (Pyrex) under an argon atmosphere. Subsequent condensation of ammonia lead to an initially colorless solution, after which the NMR tube was sealed shut by melting under an ammonia atmosphere. The sample was stored at 193 K until examination by NMR spectroscopy.

Synthesis of (NHC^{tBu}Au)$_3$NHCl and [(NHC^{tBu}Au)$_6$(η^2-Si$_4$)]Cl$_2$·7NH$_3$: $Rb_6Cs_6Si_{17}$ (150 mg, 0.08 mmol) and NHC^{tBu}AuCl (34.6 mg, 0.08 mmol) with [2.2.2]-cryptand (47.4 mg, 0.13 mmol) as a chelating agent were weighed into a heated Schlenk tube under argon atmosphere and subsequently approximately 5 mL of ammonia were condensed onto the reactants. After six weeks of storage at 233 K, yellow crystals of **1** could be isolated from the slightly reddish solution as the main product, as well as one orange-red crystal of **2**, and characterized by single-crystal X-ray diffraction.

X-ray Crystal Structure Determination: Perfluorether oil was cooled in a stream of liquid nitrogen and crystals were transferred from the cooled reaction vessel into the oil under argon counter current. Suitable crystals were scooped up on MiTeGen holders and transferred onto the diffractometer in liquid nitrogen. Both crystals were measured on a diffractometer SuperNova by the company Agilent, equipped with a molybdenum micro focus tube. Data reductions were performed using the software CrysAlisPro 39.37b.[42] The software Olex2-1.2-alpha,[43] as well as the programs ShelXS and ShelXT were used for structure solution,[44] ShelXL for the refinement.[45] For visualization Diamond 4 was employed.[46]

Further details of the crystal structures investigations may be obtained from the Fachinformationszentrum Karlsruhe, 76344 Eggenstein-Leopoldshafen, Germany (Fax: +49-7247-808-666; E-Mail: crysdata@fiz-karlsruhe.de, http://www.fiz-karlsruhe.de/request for deposited data.html) on quoting the depository numbers CSD-1954886 for **1** and CSD-1957884 for **2**.

NMR Studies: NMR spectra were recorded on a Bruker Avance III HD 600 MHz spectrometer equipped with a fluorine selective TBIF probe and a Bruker Avance NEO 600 MHz spectrometer equipped with a double resonance broad band probe (BBO). ^{1}H, ^{13}C and ^{29}Si-NMR spectra were referenced externally to TMS (tetramethylsilane). In case the ^{29}Si signal of the HSi_9^{3-} was detected, the spectra were calibrated on the literature known chemical shift of HSi_9^{3-} (–358.5 ppm). ^{15}N-NMR spectra were referenced externally to NH_3. The temperature (233 K) for measurements at Bruker Avance NEO was controlled by a Bruker BVTE 3000 temperature unit. The temperatures (203–233 K) for measurements at Bruker Avance III HD were controlled by a Bruker BVTE 3900 temperature unit. Data was processed with the Bruker software TOPSPIN 3.2 and TOPSPIN 4.0.7. For spectra and assignments see Supporting Information.

Computational Details: DFT calculations were performed using the software package ORCA 4.0,[47] which also has an interface for the NBO 6 program.[48] ELF calculations were performed with MultiWFN,[49] obtained attractors were evaluated with Avogadro,[50] and 3D isosurface pictures were created with Molekel.[51]

Supporting Information (see footnote on the first page of this article): Additional information on the crystallographic, computational and NMR data is provided in the Supporting Information.

Acknowledgements

We gratefully acknowledge financial support from the German Science Foundation (DFG) (KO 1857/10–1, and GS 13/5–1). Open access funding enabled and organized by Projekt DEAL.

Keywords: Liquid ammonia; Zintl phases; NMR spectroscopy; Silicide; Reactivity; Gold

References

[1] H. Schmidbaur, A. Schier, *Chem. Soc. Rev.* **2008**, *37*, 1931–1951; H. Schmidbaur, A. Schier, *Chem. Soc. Rev.* **2012**, *41*, 370–412.

[2] K. Angermaier, H. Schmidbaur, *J. Chem. Soc., Dalton Trans.* **1995**, 559–564; J. M. López-de-Luzuriaga, A. Sladek, A. Schier, H. Schmidbaur, *Inorg. Chem.* **1997**, *36*, 966–968; U. M. Tripathi, W. Scherer, A. Schier, H. Schmidbaur, *Inorg. Chem.* **1998**, *37*, 174–175.
[3] V. Ramamoorthy, P. R. Sharp, *Inorg. Chem.* **1990**, *29*, 3336–3339; V. Ramamoorthy, Z. Wu, Y. Yi, P. R. Sharp, *J. Am. Chem. Soc.* **1992**, *114*, 1526–1527; X. He, Y. Wang, H. Jiang, L. Zhao, *J. Am. Chem. Soc.* **2016**, *138*, 5634–5643.
[4] D. Marchione, L. Belpassi, G. Bistoni, A. Macchioni, F. Tarantelli, D. Zuccaccia, *Organometallics* **2014**, *33*, 4200–4208.
[5] S. Scharfe, F. Kraus, S. Stegmaier, A. Schier, T. F. Fässler, *Angew. Chem. Int. Ed.* **2011**, *50*, 3630–3670; S. C. Sevov, J. M. Goicoechea, *Organometallics* **2006**, *25*; J. M. Goicoechea, S. C. Sevov, *J. Am. Chem. Soc.* **2006**, *128*, 4155–4161.
[6] J. M. Goicoechea, S. C. Sevov, *Organometallics* **2006**, *25*, 4530–4536.
[7] S. Joseph, M. Hamberger, F. Mutzbauer, O. Hartl, M. Meier, N. Korber, *Angew. Chem. Int. Ed.* **2009**, *48*, 8770–8772.
[8] F. S. Geitner, T. F. Fässler, *Chem. Commun.* **2017**, *53*, 12974–12977.
[9] M. Waibel, F. Kraus, S. Scharfe, B. Wahl, T. F. Fässler, *Angew. Chem. Int. Ed.* **2010**, *49*, 6611–6615.
[10] A. Spiekermann, S. D. Hoffmann, T. F. Fässler, I. Krossing, U. Preiss, *Angew. Chem. Int. Ed.* **2007**, *46*, 5310–5313; A. Spiekermann, S. D. Hoffmann, F. Kraus, T. F. Fässler, *Angew. Chem. Int. Ed.* **2007**, *46*, 1638–1640; F. S. Geitner, T. F. Fässler, *Eur. J. Inorg. Chem.* **2016**, 2688–2691; L. J. Schiegerl, F. S. Geitner, C. Fischer, W. Klein, T. F. Fässler, *Z. Anorg. Allg. Chem.* **2016**, *642*, 1419–1426; C. Schenk, A. Schnepf, *Angew. Chem. Int. Ed.* **2007**, *46*, 5314–5316.
[11] F. S. Geitner, W. Klein, T. F. Fässler, *Dalton Trans.* **2017**, *46*, 5796–5800; L.-J. Li, F.-X. Pan, F.-Y. Li, Z.-F. Chen, Z.-M. Sun, *Inorg. Chem. Front.* **2017**, *4*, 1393–1396.
[12] S. Mohapatra, Y. K. Mishra, D. K. Avasthi, D. Kabiraj, J. Ghatak, S. Varma, *Appl. Phys. Lett.* **2008**, *92*, 103105; H. Zhang, Y. Zhu, L. Qu, H. Wu, H. Kong, Z. Yang, D. Chen, E. Mäkilä, J. Salonen, H. A. Santos, M. Hai, D. A. Weitz, *Nano Lett.* **2018**, *18*, 1448–1453; S. Kutrovskaya, S. Arakelian, A. Kucherik, A. Osipov, A. Evlyukhin, A. V. Kavokin, *Sci. Rep.* **2017**, *547*, 10284.
[13] M. Neumeier, F. Fendt, S. Gaertner, C. Koch, T. Gaertner, N. Korber, R. M. Gschwind, *Angew. Chem. Int. Ed.* **2013**, *52*, 4483–4486.
[14] F. Hastreiter, C. Lorenz, J. Hioe, S. Gärtner, N. Lokesh, N. Korber, R. Gschwind, *Angew. Chem.* **2019**, *131*, 3165–3169.
[15] C. Lorenz, F. Hastreiter, J. Hioe, N. Lokesh, S. Gärtner, N. Korber, R. M. Gschwind, *Angew. Chem. Int. Ed.* **2018**, *57*, 12956–12960.
[16] C. Lorenz, S. Gartner, N. Korber, *Z. Anorg. Allg. Chem.* **2017**, *643*, 141–145.
[17] T. Henneberger, W. Klein, J. V. Dums, T. F. Fässler, *Chem. Commun.* **2018**, *54*, 12381–12384.
[18] N. Wiberg, C. M. M. Finger, K. Polborn, *Angew. Chem. Int. Ed. Engl.* **1993**, *32*, 1054–1056.
[19] P. Pyykkö, *J. Phys. Chem. A* **2015**, *119*, 2326–2337.
[20] T. Müller, in *Organosilicon Chemistry IV: From Molecules to Materials, Vol. 1* (Eds.: N. Auner, J. Weis), Wiley-VCH, **2000**, pp. 110–117.
[21] A. Wiesner, S. Steinhauer, H. Beckers, C. Müller, S. Riedel, *Chem. Sci.* **2018**, *9*, 7169–7173.
[22] J. D. Corbett, D. G. Adolphson, D. J. Merryman, P. A. Edwards, F. J. Armatis, *J. Am. Chem. Soc.* **1975**, *97*, 6267–6268.
[23] M. V. Baker, P. J. Barnard, S. J. Berners-Price, S. K. Brayshaw, J. L. Hickey, B. W. Skelton, A. H. White, *Dalton Trans.* **2006**, 3708–3715.
[24] A. Collado, A. Gomez-Suarez, A. R. Martin, A. M. Z. Slawin, S. P. Nolan, *Chem. Commun.* **2013**, 5541–5543.
[25] M. Alcarazo, T. Stork, A. Anakuthil, W. Thiel, A. Fürstner, *Angew. Chem. Int. Ed.* **2010**, *49*, 2542–2546; M. V. Baker, P. J. Barnard, S. K. Brayshaw, J. L. Hickey, B. W. Skelton, A. H. White, *Dalton Trans.* **2005**, 37–43.
[26] S. Patil, A. Deally, F. Hackenberg, L. Kaps, H. Müller-Bunz, R. Schobert, M. Tacke, *Helv. Chim. Acta* **2011**, *94*, 1551–1562.
[27] E. C. Hurst, K. Wilson, I. J. S. Fairlamb, V. Chechik, *New J. Chem.* **2009**, *33*, 1837–1840.
[28] J. W. Runyon, O. Steinhof, H. V. Rasika Dias, J. C. Calabrese, W. J. Marshall, A. J. Arduengo III, *Aust. J. Chem.* **2011**, *64*, 1165–1172.
[29] I. A. Shkrob, *J. Phys. Chem. B* **2010**, *114*, 368–375.
[30] H. Ibrahim, R. Guillot, F. Cisnetti, A. Gautier, *Chem. Commun.* **2014**, *50*, 7154–7156.
[31] R. S. Ramon, S. Gaillard, A. Poater, L. Cavallo, A. M. Z. Slawin, S. P. Nolan, *Chem. Eur. J.* **2011**, *17*, 1238–1246.
[32] N. M. Scott, R. Dorta, E. D. Stevens, A. Correa, L. Cavallo, S. P. Nolan, *J. Am. Chem. Soc.* **2005**, *127*, 3516–3526.
[33] H.-W. Wanzlick, E. Schikora, *Chem. Ber.* **1961**, *94*, 2389–2393; H.-W. Wanzlick, E. Schikora, *Angew. Chem.* **1960**, *72*, 494–494.
[34] P. I. Jolly, S. Zhou, D. W. Thomson, J. Garnier, J. A. Parkinson, T. Tuttle, J. A. Murphy, *Chem. Sci.* **2012**, *3*, 1675–1679.
[35] $H^{4,5}$ of **11** may be assigned to one of the signals around **7** which we assume to belong to NHC$^{r\mathrm{Bu}}$ species with a chemical environment similar to **7** which would be the case for **11**.
[36] A. N. Nesmeyanov, E. G. Perealova, Y. T. Struchkov, M. Y. Antipin, K. I. Grandberg, V. P. Dyadhenko, *J. Organomet. Chem.* **1980**, *201*, 343–349.
[37] A. Bauer, F. Gabbai, A. Schier, H. Schmidbaur, *Philos. T. R. Soc. A* **1996**, *354*, 381–394.
[38] A. J. Bellamy, W. S. J. P. Golding, *Propellants Explos. Pyrotech.* **2002**, *27*, 59–61.
[39] R. A. J. Ogg, *J. Chem. Phys.* **1954**, *22*, 560–561.
[40] NH_4^+ was detected in sample **ii** at 203 K evidenced by a characteristic triplet[38] at δ = 7.02 ppm; J = 51.5 Hz; ^{14}N: spin = 1; similar pattern for ^{1}H-NMR signal of dry ammonia].[39]
[41] H. Bürger, R. Eujen, H. C. Marsmann, *Z. Naturforsch. B* **1947**, *29*, 149–152.
[42] Agilent Technologies, Santa Clara, CA, USA, **2017**.
[43] O. V. Dolomanov, L. J. Bourhis, R. J. Gildea, J. A. K. Howard, H. Puschmann, *J. Appl. Crystallogr.* **2009**, *42*, 339–341.
[44] G. M. Sheldrick, *Acta Crystallogr., Sect. A* **2008**, *64*, 112–122; G. M. Sheldrick, *Acta Crystallogr., Sect. A* **2015**, *71*, 3–8.
[45] G. M. Sheldrick, *Acta Crystallogr., Sect. C* **2015**, *71*, 3–8.
[46] K. Brandenburg, **2018**; K. Brandenburg, *Vol. Version 3.2k*, Crystal Impact GbR, Bonn, Germany, **2014**.
[47] F. Neese, *Wiley Interdiscip. Rev. Comput. Mol. Sci.* **2017**, *8*, e1327; F. Neese, *Wiley Interdiscip. Rev. Comput. Mol. Sci.* **2012**, *2*, 73–78.
[48] E. D. Glendening, C. R. Landis, F. Weinhold, *J. Comput. Chem.* **2013**, *34*, 1429–1437.
[49] T. Lu, F. Chen, *J. Comput. Chem.* **2012**, *33*, 580–592.
[50] M. D. Hanwell, D. E. Curtis, D. C. Lonie, T. Vandermeersch, E. Zurek, G. R. Hutchison, *J. Cheminformatics* **2012**, *4*.
[51] U. Varetto, **2009**.

Received: July 23, 2020